

The Method of Time-Resolved Spin-Probe Oximetry: Its Application to Oxygen Consumption by Cytochrome *c* Oxidase[†]

Jinjie Jiang,[‡] Janet F. Bank,[‡] Weiwen Zhao,[‡] and Charles P. Scholes*

Department of Chemistry, State University of New York at Albany, Albany, New York 12222

Received August 6, 1991; Revised Manuscript Received October 30, 1991

ABSTRACT: This work broadens the scope and improves the time resolution of spin-probe oximetry, a technique in which small nitroxide spin probes detect oxygen consumption via change in their relaxation properties [Froncisz, W., Lai, C.-S., & Hyde, J. S. (1985) *Proc. Natl. Acad. Sci. U.S.A.* 82, 411-415]. For rapid oxygen kinetic studies we combined the methodology of spin-probe oximetry with a recently developed loop-gap resonator, stopped-flow EPR system [Hubbell, W. L., Froncisz, W., & Hyde, J. S. (1987) *Rev. Sci. Instrum.* 58, 1879-1886]. The technique used microliter volumes of reactant solutions. Enzymatic consumption of oxygen by cytochrome *c* oxidase in the presence of ferrocytochrome *c* substrate was followed continuously in time under limited-turnover conditions, where the concentration of oxygen consumed often was comparable to or less than the amount of enzyme present. In detecting less than micromolar oxygen concentration changes, we have achieved a time resolution of the order 30 ms when flow is stopped. Oxygen consumption was followed under two different limited-turnover conditions: In the first, the amount of oxygen consumed was limited by available ferrocytochrome *c*, and the time course of oxygen consumption and its pH dependence were compared with the optically detected ferrocytochrome *c* consumption. In the second, the oxygen consumed was ultimately limited by the availability of oxygen itself while ferrocytochrome *c* was regenerated and remained in excess. The overall amount of oxygen consumed was of the order of 10 times the amount of enzyme, and more rapid oxygen consumption was observed for enzyme in the prereduced "pulsed" form [Antonini, E., Brunori, M., Greenwood, C., Colosimo, A., & Wilson, M. T. (1977) *Proc. Natl. Acad. Sci. U.S.A.* 74, 3128-3132] than in the "resting" form. These latter oxygen-limited experiments showed a zeroth-order rate dependence on oxygen concentration down to an oxygen concentration of less than 1 μ M. Below 1 μ M oxygen, where oxygen itself became rate limiting, our technique enabled us to observe the oxygen consumption rate diminish to zero in a period of less than 1 s and to estimate the oxygen concentration where the rate diminished to half-maximal value.

Cytochrome *c* oxidase (CcO)¹ takes four electrons from ferrocytochrome *c* (cyt *c*²⁺) and combines them in sequential fashion with oxygen to provide H₂O. Such electrons are thought to be initially transferred to the metal centers cytochrome *a* and Cu_A and thence to the a₃-Cu_B binuclear center, where oxygen is catalyzed to water. In the mitochondrial setting this electron-transfer process is coupled to transmembrane proton pumping (Wikström et al., 1981; Malmström, 1985, 1990; Malmström & Nilsson, 1988).

CcO has in effect two substrates, reduced cyt *c*²⁺ and oxygen. (If one considers the protons that are consumed in creating water or are pumped, there are actually three substrates.) In probing CcO kinetics under limited-turnover conditions, where finite ratios of substrate to enzyme hold, researchers have generally followed the transient spectrophotometric changes of cyt *c*²⁺ or of chromophores in the oxidase itself (Gibson & Greenwood, 1963; Hill & Greenwood, 1983). Consumption of oxygen at the a₃-Cu_B center leads to complicated behavior as oxygen is bound and then converted through several short-lived intermediates to H₂O. This behavior has also been followed optically by cryogenic freeze trapping (Chance et al., 1975) or more recently by time-resolved resonance Raman techniques (Babcock et al., 1984; Han et al., 1990; Ogura et al., 1990). Changes of the overlapped

cytochrome *a* and cytochrome a₃ spectra are not easily assigned even under equilibrium conditions (Hendler et al., 1986), let alone kinetic ones. Therefore, we believed that a useful new tool for studying CcO would be one which would report rapid consumption of limited amounts of oxygen in analogy to the way in which the cyt *c*²⁺ optical absorbance change reports transient cyt *c*²⁺ consumption.

To achieve good time resolution of oxygen changes with minimal quantities of reacting solution, we have taken a recently reported stopped-flow EPR technique (Hubbell et al., 1987) and applied it to spin-probe oximetry methodology (Lai et al., 1982; Froncisz et al., 1985). Two appropriate classes of experiments, in which oxygen measurements would be complementary to the results of other methods, were as follows: First, experiments were performed where the amount of oxygen consumed was comparable to the amount of CcO and was limited by the amount of available and exhaustible cyt *c*²⁺. The oxygen consumption in this first type of experiment was complementary to cyt *c*²⁺ consumption. Second, experiments were performed where cyt *c*²⁺ continued to be in excess because it was being regenerated but where oxygen concentration itself

[†] This work was supported in part by American Heart Association Grant 88010410 (C.P.S.) and NIH Grant GM 35103 (C.P.S.).

* Author to whom correspondence should be addressed.

[‡] Present address: Department of Physics, State University of New York at Albany, Albany, NY 12222.

¹ Abbreviations: CcO, cytochrome *c* oxidase; cyt *c*²⁺, ferrocytochrome *c*; cyt *c*³⁺, ferricytochrome *c*; CTPO, 2,2,5,5-tetramethyl-1-oxy-3-pyrroline-3-carboxamide; TMPD, *N,N,N',N'*-tetramethyl-*p*-phenylenediamine; Hepes, 4-(2-hydroxyethyl)-1-piperazineethanesulfonic acid; TEMPONE, 2,2,6,6-tetramethyl-4-oxo-1-piperidinyloxy; Tween 20, poly(oxyethylene)sorbitan monolaurate; i.d., inside diameter; o.d., outside diameter; LGR, loop-gap resonator; χ'' , absorption; χ' , dispersion; mV, millivolt; p.t.p., peak to peak.

became limiting. These would be complementary to slower polarographic experiments. These latter experiments also gave us the opportunity to compare the rate of oxygen consumption for CcO which had been prereduced and put into its more active "pulsed" form with the rate from oxidase which had not seen prereduction and was still in its less active "resting" form (Antonini et al., 1977; Brunori et al., 1979).

The relaxation times of freely tumbling nitroxide spin probes are sensitive to oxygen concentration. The technique of monitoring oxygen consumption through the nitroxide radical signal is called spin-probe oximetry (Lai et al., 1982; Froncisz et al., 1985). Molecular collisions between spin probe and paramagnetic oxygen modulate the Heisenberg exchange between probe spin and the triplet oxygen molecule (Povich, 1975; Windrem & Plachy, 1980; Subczynski & Hyde, 1981), they generally enhance the probe's magnetic T_1 and T_2 relaxation, and they broaden its standard peak-to-peak first derivative absorption ($d\chi''/dH$) EPR signal measured at low powers. Our pilot time-resolved spin-probe oximetry on oxygen consumption by CcO used absorption EPR with a standard-flow flat cell and rudimentary stopping system (Scholes et al., 1987), and this work focused us on improving sensitivity, diminishing reagent usage, and improving time resolution through more modern devices which were just being reported (Hubbell et al., 1987).

The saturation and saturation-transfer properties of the spin probe are also sensitive to oxygen-induced changes in its T_1 (Froncisz et al., 1985). An increase in oxygen concentration will decrease T_1 , and a decrease in T_1 will increase the saturated dispersion signal, especially if it is observed while using 100-kHz field modulation and 90°-out-of-phase detection (Froncisz et al., 1985). The dispersion method exhibited higher sensitivity and showed linearity in its response to oxygen concentration at oxygen concentrations below 100 μM (<50% air-saturated buffer).

Because of its much greater filling factor, small size, insensitivity to dielectric losses, and lower Q factor, a loop-gap resonator (LGR) (Froncisz & Hyde, 1982) is preferable for small liquid samples, especially where T_1 -sensitive dispersion methods are used (Froncisz et al., 1985). The LGR has been used to monitor oxygen consumption by a small number of living cells suspended in a 5- μL volume (Froncisz et al., 1985). In another LGR application Hubbell et al. (1987) integrated an X-band loop-gap resonator with sample volume of 1.5 μL to an Update Instruments Wiskind grid mixing chamber and Ram Driver. The Ram Driver was precisely programmed through its stepping motor to drive and stop microliter quantities of reactants so that the transients from numerous small-volume shots could be averaged. In that stopped-flow EPR work the decay of free radicals having half-lives of the order of several hundred milliseconds was observed following mixing of reactants.

Our technique contrasts with the standard polarographic method for measuring oxygen concentration that uses the Clark oxygen electrode (Davies, 1962). The polarographic method for measuring oxygen consumption is generally a steady-state method that uses minuscule amounts of enzyme compared to the oxygen consumed, and its time resolution is limited by stirring and by diffusion through the membrane that covers the oxygen electrode. Without a membrane, "aging" of the electrode surface causes loss of sensitivity (Davies, 1962). A more recently reported method of oxygen determination used the oxygen-sensitive phosphorescence lifetime of certain "luminophores" (Vanderkooi et al., 1987; Wilson et al., 1988). This technique has high absolute sensitivity for measuring

oxygen concentrations below 1 μM , and it has the additional advantage that cyt c^{2+} concentration could be simultaneously monitored. The phosphorescence lifetime method was reported to give a measure of the oxygen concentration in less than 100 ms, but the repetition rate for such oxygen measurements was 2 s^{-1} (Wilson et al., 1988). Such a slow repetition rate (meaning a long time between oxygen measurements) would limit the capability for continuously and rapidly monitoring oxygen concentration. The cuvette used for these phosphorescence measurements held a volume of the order of 1 mL, and reagents were introduced into it by Hamilton syringe and mixed by a magnetic stirrer rather than by a rapid mixing device (Wilson et al., 1988). As reported, the phosphorescence lifetime method would appear excellent for measuring absolute oxygen concentrations and the concomitant cyt c^{2+} levels on fairly large volume samples, but not for continuously measuring subsecond oxygen kinetics on microliter samples.

Over the last decade we have used EPR and ENDOR (electron nuclear double resonance) under cryogenic conditions to understand the *structure* of cytochrome a , Cu_A , and cytochrome a_3 (Stevens et al., 1982; Mascarenhas et al., 1983; Martin et al., 1985; Fan et al., 1988). We now use EPR as a probe for CcO *function* under near-physiological conditions. Spin-probe oximetry methodology continues to be of importance in following oxygen consumption in cellular physiology (Swartz & Glockner, 1989). The nitroxide-based EPR oximetry has shown potential for measuring oxygen concentration changes on the millisecond time scale when oxygen evolution was initiated by short light pulses upon photosynthetic systems contained in a standard EPR flat cell (Strzalka et al., 1990). CcO is of intrinsic interest to us and others because it is the major oxygen-consuming enzyme in cellular metabolism. Stopped-flow EPR should become an important new technique now that small resonant structures like the LGR are available. Thus the purpose of this work was to broaden the scope of spin-probe oximetry, to probe CcO's oxygen-consuming function, and to develop stopped-flow EPR.

EXPERIMENTAL PROCEDURES

Materials. Beef heart CcO (ferrocytochrome $c:\text{O}_2$ oxidoreductase; EC 1.9.3.1) was prepared by the methods of King and co-workers (Kuboyama et al., 1972; Yu et al., 1975). Partially purified starting material, obtained at the point where CcO is separated from other mitochondrial proteins, was kindly provided by Prof. C.-A. Yu, Department of Biochemistry, Oklahoma State University. In determining concentrations of CcO, we used a difference millimolar extinction coefficient of $\Delta\epsilon_{\text{red-ox}} = 24 \text{ mM}^{-1} \text{ cm}^{-1}$ per CcO molecule at 605 nm (Jensen et al., 1981). Aliquots from a single CcO enzyme preparation, suspended in buffers containing Tween 20 detergent (specially purified, Pierce Chemical), were used for all measurements. Enzyme purity and activity were checked by optical and polarographic methods detailed in the Biochemical Methods section of Fan et al. (1988). The nitroxide spin probe used for spin-probe oximetry was CTPO (Sigma), whose structure is shown in the inset to Figure 1. CTPO at 200 μM concentration had no effect on enzyme oxygen consumption as measured polarographically or on cyt c^{2+} consumption as measured by optical stopped flow. In our initial work we used CTPO probe containing naturally abundant ^{14}N and ^1H , but we subsequently found that the ^{15}N -perdeuterated form of CTPO (MSD Isotopes, Point Claire-Dorval, Quebec) improved the spin-probe oximetry signal and signal to noise by at least a factor of 2. Cytochrome c (type VI horse heart, Sigma) was reduced with 2 mM ascorbate, then chromatographed on a Sephadex G-25 column to remove ascorbate, and

stored frozen at about 1 mM concentration in liquid nitrogen. To determine cyt c^{2+} consumption, we used a difference millimolar extinction coefficient for cyt c of $\Delta\epsilon_{\text{red-ox}} = 21 \text{ mM}^{-1} \text{ cm}^{-1}$ at 550 nm (Jensen et al., 1981).

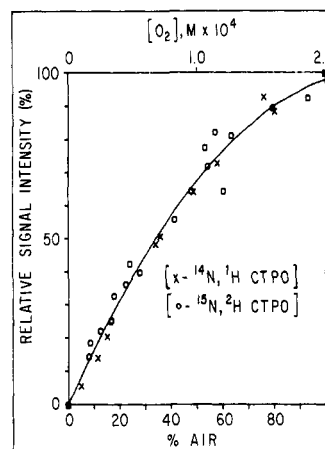
Where rapid regeneration of cyt c^{2+} was needed to allow complete consumption of oxygen, concentrations after mixing of 1 mM ascorbate and 200 μM TMPD (Sigma) were used. Although ascorbate will quickly reduce nitroxide spin probes like TEMPONE at high pH and high ascorbate concentration (see Figure 2B), the half-time at neutral pH for reduction of 200 μM CTPO probe was 1 h in the presence of the 1 mM ascorbate, 200 μM TMPD, and 40 μM cyt c^{2+} that are used as reductants in many of these experiments.

As part of the oximetry calibration procedure, we consumed oxygen by mixing glucose oxidase (EC 1.1.3.4, 24 units/mg, type II, Sigma) at a concentration of 0.1 mg/mL and beef heart catalase at 0.1 mg/mL (EC 1.11.1.6; 1600 units/mg, Sigma) with 12 mM glucose (Gibson et al., 1964).

Methods. Our EPR spectrometer was a Bruker ER 200-D SRC spectrometer with Model ER 023 absorption/dispersion X-band bridge. To obtain at least a 2-fold improvement of signal to noise, a MITEQ Model AMF-2S-8596-4 low-noise 15-dB GASFET amplifier (MITEQ Inc., Hauppauge, NY) was incorporated before the crystal detector in the Bruker bridge (Hubbell et al., 1987). Data were collected by an AT&T Model 6300 computer fitted with an IBM DAC card and the EW 2.23 (Morse, 1987) EPR software package (Scientific Sales Systems, Bloomington, IL). This software contained a triggerable fast-scan mode to collect transient spin-probe EPR signals. A Nicolet Model 12/70 signal averager was also used for monitoring the transient EPR signal during and after flow stoppage.

We used an X-band loop-gap resonator manufactured by Medical Advances (Milwaukee, WI). This LGR was specifically made to interface to an Update Instruments (Madison, WI) Wiskind grid mixer after the fashion reported by Hubbell et al. (1987). A 0.6 mm i.d., 0.8 mm o.d. quartz tube carried the sample mixture from the mixer up through the LGR. The dead volume of 5.6 μL was the volume of the 2-cm length of this tube between mixer and LGR, where the volume of the 5 mm long tube actually within the LGR is approximately 1.5 μL . An Update Instruments Model 715 syringe ram controller (Madison, WI) drove reactants from two syringes through thick-walled nylon tubes to the mixer. The effective dead time for the stopped-flow system, which includes the 15-ms braking time for the ram, was computed to be 18 ms using Formula A1² in the appendix of Hubbell et al. (1987). An electronic pulse provided by the ram driver at the start of its braking cycle was used for triggering our data-collecting apparatus.

For both the ^{14}N -protonated and the ^{15}N -perdeuterated CTPO probes we calibrated voltage changes of the 90°-out-of-phase dispersion EPR signal vs percent air at the gain settings, modulation amplitudes, and powers indicated in the legend to Figure 1. This work was done, as was all the subsequent kinetic work, at an ambient temperature of 21 ± 1 °C. The magnetic field was set on the center of the middle ^{14}N nitrogen hyperfine line or on the center of the higher field ^{15}N nitrogen hyperfine line, and the height of that feature was monitored and compared with the corresponding heights at 0% and 100% air (Froncisz et al., 1985). Solutions were



$^{14}\text{N}, ^1\text{H}$ CTPO - 100% SIGNAL = 6.6 V

$^{15}\text{N}, ^2\text{H}$ CTPO - 100% SIGNAL = 7.5 V

FIGURE 1: Calibration chart of the relative 90°-out-of-phase dispersion signal intensity vs percent (%) ambient air from 0% to 100% ambient air. The curve was the least-squares-fitted curve to an expression (eq 1) containing a linear and a quadratic term in percent (%) ambient air; the linear term predominates below 30% ambient air. One hundred percent ambient air corresponded to $200 \pm 20 \mu\text{M}$ oxygen concentration.³ The phase of the 100-kHz detector was set for 0 V at 0% air as determined when glucose and glucose oxidase had finished consuming all the oxygen within the quartz sample tube. For the ^{14}N -protonated spin probe the modulation = 1.0 G p.t.p., gain = 1.25×10^4 , power = 6.0 mW, and the 0%-100% signal change was 6.6 ± 0.6 V. For the ^{15}N -perdeuterated spin probe the modulation = 0.63 G p.t.p., gain = 8×10^3 , power = 2.0 mW, and the 0%-100% signal change was 7.5 ± 0.6 V. The inset shows the structure of CTPO.

prepared with known percentages of oxygen by mixing air-saturated and helium-degassed buffer. These solutions were slowly flowed through the LGR, their signals were recorded, and the oxygen concentration was continuously monitored by a micro oxygen electrode³ (Microelectrodes, Inc., Londonderry, NH) placed in the flow line after the LGR. The signal intensity obtained from these experiments was compared to the 100% ambient air signal and to the 0% ambient air signal to provide a relative signal intensity. The 0% ambient air signal and the EPR signal change between 100% and 0% ambient air were independently and repeatedly monitored during the course of the calibration, and routinely during kinetic measurements, by observing the overall signal change after mixing glucose and glucose oxidase. As Figure 1 shows, the change of signal with oxygen concentration (i.e., slope of the curve) was somewhat higher and approximately linear below about 30% ambient air or 60 μM oxygen. The calibration curve of the relative signal intensity vs percent ambient air was very similar to that reported by Froncisz et al. (1985), and these workers specifically determined a linear relation between signal change and oxygen below 20 μM oxygen concentration. The calibration curve in Figure 1 was fit to an empirical expression:

$$y = ax + bx^2 \quad (1)$$

where y = percent (%) signal change and x = percent (%) ambient atmospheric oxygen. The least-squares fit gave $a = 1.72 \pm 0.05$ and $b = (-7.45 \pm 0.73) \times 10^{-3}$. The slope of the calibration curve is $dy/dx = a + 2bx$, from which the sensitivity of the spin-probe oximetry method to small changes in oxygen concentration can be calculated. The slope, dy/dx ,

² The relevant quantities in this calculation are the 0.8 cm/s ram driver speed, the 0.33-cm² cross-sectional area of each syringe, the 15-ms braking time for the ram (as determined from the optical encoder pulses of the ram driver), a capillary dead volume of 5.6 μL , and a braking displacement of 0.006 cm.

³ The microelectrode indicated that on the average 100% air corresponded to a 200 μM concentration of oxygen. The day-to-day fluctuation in this concentration was approximately $\pm 10\%$.

has units of (% signal change)/(% atmospheric oxygen). This slope can be converted to (mV signal)/($\mu\text{M O}_2$) by first multiplying dy/dx by the overall EPR signal difference obtained between 0% and 100% ambient air (this difference was 7500 mV for the ^{15}N -perdeuterated CTPO and 6600 mV for the ^{14}N -protonated CTPO) and then dividing by the micromolar concentration of oxygen that is contained in 100% ambient air (this concentration was 200 μM oxygen according to our in-line oxygen electrode). For the ^{15}N -perdeuterated and the ^{14}N -protonated CTPO we thus would respectively obtain a sensitivity of 65 and 57 (mV signal)/($\mu\text{M O}_2$) near 0% ambient air and 48 and 42 (mV signal)/($\mu\text{M O}_2$) at 30% ambient air. Due to the higher signal sensitivity at lower oxygen concentrations, we did most of our work in the EPR dispersion mode at concentrations at or below 30% ambient air. Under the same instrumental settings (Figure 1 legend) which gave these sensitivities, the p.t.p. noise level was about 20 mV with a 10-ms time constant.

For the T_1 -sensitive dispersion method it was necessary to look for changes in the 90° -out-of-phase 100-kHz field-modulated signal. This signal is a minimal signal with respect to the large in-phase dispersion signal. Fortunately, the magnitude of the oxygen-induced signal change, say, between 0% and 100% ambient air-saturated buffer, was not extremely sensitive to the exact phase setting. We determined that over a phase range of $\pm 10^\circ$ about the 90° set point the oxygen-induced change in signal is approximately independent of the initial phase setting. This meant that our time-resolved work was not sensitive to minor phase drifts which can occur over a period of several hours. (During calibration procedures we also devised a method to monitor phase drift in the reference phase of the Bruker 100-kHz amplifier through the use of a second independent phase-sensitive detector.)

In order to correlate our results with standard stopped-flow measurements of cyt c^{2+} consumption, we performed optically detected stopped-flow measurements with an Aminco-Murrow stopped-flow attachment coupled to a DW-2 (SLM Instruments, Urbana, IL) UV-vis spectrophotometer. This 1972 vintage spectrophotometer had been computer-interfaced and upgraded by On Line Instrument Systems, Inc. (Jefferson, GA), and we used the OLIS stopped-flow package in taking and plotting optical stopped-flow data.

RESULTS AND DISCUSSION

We tested both the low-power (0.2 mW) absorption oximetry method (Lai et al., 1982) and the higher power (>1 mW) dispersion technique (Froncisz et al., 1985). The overall signal change between 0% and 100% ambient atmospheric oxygen was 10 times larger for the dispersion method, and the signal to noise for such a change was 5 times larger by the dispersion method. Hence, we settled on using the dispersion method, whose signal to noise increased by another factor of 2 when we used ^{15}N -perdeuterated CTPO instead of ^{14}N -protonated CTPO.

Results: Rapid Measurements following Mixing. Considerable effort was made to minimize the transient overshoots, undershoots, or in general "glitches", especially those which could occur when flow was stopped. The overshoot reported by Hubbell et al. (1987) was of the order of 10% of the signal amplitude. When we first started measurements, our transient when stopping in spin-probe oximetry measurements was of the order of 0.5 V. R. Hansen of Update Instruments made modifications to the mixer-LGR combination to *precisely and rigidly* hold the quartz sample flow tube within the critical loop of the LGR. It was good practice to have fresh O-rings throughout the system and to be sure the drive syringes were

free of bubbles which would lead to transients during their compression and decompression. Transparent syringe bodies enabled one to detect bubbles. With these modifications and precautions the transient height was diminished from 500 mV to about 100 mV. A high-pass electronic filter was placed between the Bruker bridge and the ER 022 100-kHz phase-sensitive detector, and this diminished the initial transient to below 20 mV. The high-pass filter, which had a low-frequency cutoff of about 260 Hz, was used to eliminate a 30–50-ms overloading transient from the microwave bridge to the 100-kHz amplifier. The EPR signal is carried at 100 kHz before demodulation and was unaffected by the high-pass filter. The removal of transients with improvement of the system is shown in Figure 2A.

To establish that we could measure without artifacts reactions going to completion over a few hundred milliseconds and significant changes occurring over <100 ms, we repeated experiments similar to those of Hubbell et al. (1987) where 25 μM TEMPONE spin probe was destroyed in the presence of 500 mM ascorbate, pH 10, over a few hundred milliseconds following mixing. (These are *definitely not* the conditions we use for spin-probe oximetry, and the 5-membered ring of CTPO with its 3–4 double bond is considerably more stable to ascorbate than TEMPONE with its unsaturated 6-membered ring.) Figure 2B, where data collection was triggered at the start of fluid flow, rather than at the start of braking, shows the decay of the radical when fluid was stopped. In this experiment the course of the signal was followed by more standard, in-phase dispersion EPR with a transient, if there is one, lasting ~ 30 ms after the start of braking; Hubbell et al. (1987) also noted such behavior. Thus the LGR stopped-flow system can measure rapid kinetics at times considerably less than 100 ms, provided the signal to noise involved with these changes is sufficient.

In Figure 2C we show the details over 2 s following mixing of CcO, reductant, and oxygen. The conditions we used were those in which prerduced oxidase in the presence of excess reductant was mixed with oxygen-containing buffer (containing about 20% ambient air) and spin probe. In Figure 2C we observed oxygen consumption with considerably better than 100-ms time resolution following mixing. The obscuring transient, if there is one, is less than 30 ms long and corresponds in height to less than 0.5 μM oxygen or 20 mV. The work shown in Figure 2 indicates primarily the present state of progress in removal of initial transients for measuring small oxygen concentration changes immediately after mixing of oxygen-consuming reactants.

Results: Oxygen Consumption Limited by Available Cyt c^{2+} . Since much information on CcO activity has been obtained by following cyt c^{2+} consumption with a finite ratio of cyt c^{2+} to CcO [e.g., Thornström et al. (1988)], these experiments were designed to follow concomitant oxygen consumption. The cyt c^{2+} was mixed with a CcO solution containing the spin probe so that immediately after mixing the concentrations were 5 μM CcO, 40 μM cyt c^{2+} , and 200 μM CTPO. These measurements started at an oxygen concentration of about 30% ambient air (~ 60 μM oxygen), which is well above the maximal 10 μM concentration change of oxygen expected to be consumed. The kinetic traces in Figure 3 indicated oxygen consumption where the signal change was limited by available cyt c^{2+} . Such changes were not observed in the presence of CcO's cyanide inhibitor. As next shown in Figure 4, we monitored the cyt c^{2+} consumption at 550 nM by optically detected stopped flow over the same time range and under the essentially the same conditions used when we

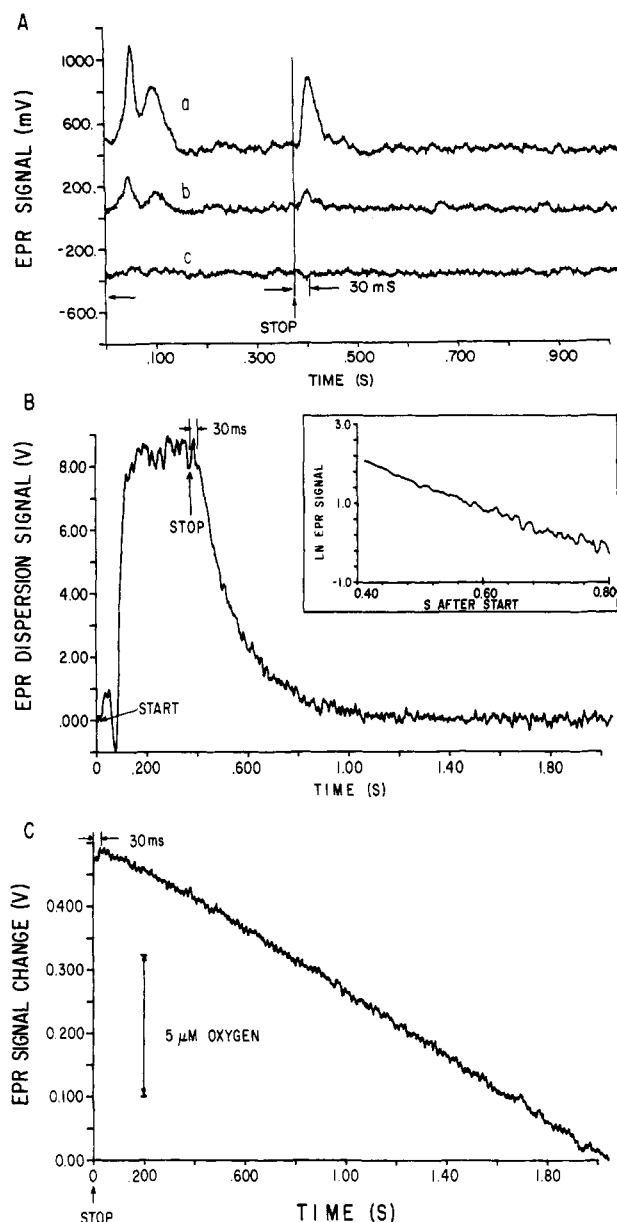


FIGURE 2: Panel A shows the size of transient artifacts from mixing 400 μM CTPO and buffer under the following conditions: (a) the mixer-flow tube was loosely assembled, and there was no high-pass filter before the 100-kHz amplifier; (b) the mixer-flow tube was tightly assembled, and there was no high-pass filter before the 100-kHz amplifier; (c) the mixer-flow tube was tightly assembled, and there was a high-pass filter before the 100-kHz amplifier. Panel B shows the rapid degradation of the spin probe TEMPONE at 25 μM concentration in the presence of 0.5 M ascorbate, pH 10.0. The signal averager was triggered at the start of the ram drive rather than the beginning of the braking cycle. The ram started to brake at the point indicated "STOP", which is 375 ms after the start of flow. The bars indicate the approximate length of the "transient" following this braking. The inset indicates the approximate first-order nature of the reaction, which had previously been noted by Hubbell et al. (1987). The gain setting was 4×10^4 , modulation 0.63 G p.t.p., power 2 mW, dispersion in phase signal, time constant = 0.005 s, and 2 ms per data point. Panel C indicates the time-resolved spin-probe oximetry signal following the mixing of "pulsed" oxidase with oxygen-containing buffer in the presence of excess reductant. After mixing, the concentration of reactants was 5 μM CcO, 40 μM cyt c^{2+} , 1 mM ascorbate, 200 μM TMPD, 60 μM oxygen, 200 μM ^{15}N -perdeuterated CTPO, 0.05 M Hepes, and 0.167 M K_2SO_4 , pH 7.0. The signal averager was triggered at the beginning of ram braking, and the curve in panel C is due to the accumulation of 10 transients, each with an instrumental time constant of 0.01 s. Instrumental settings are as in the legend for Figure 1. Approximate time for the 30-ms transient is shown. Signal averager used 2 ms/address.

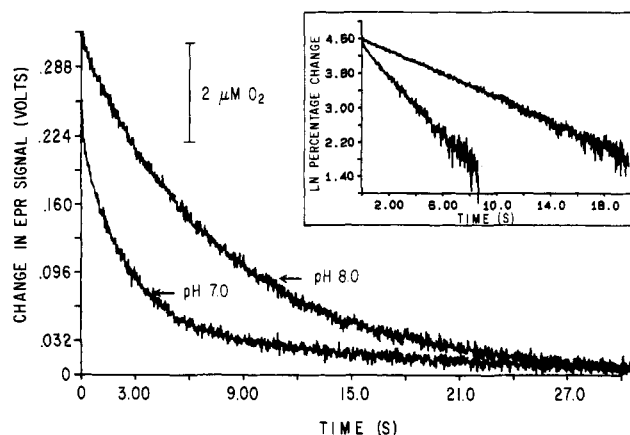


FIGURE 3: Time-resolved spin-probe oximetry signal from the ^{15}N -perdeuterated CTPO under conditions where limited cyt c^{2+} in turn limited the oxygen consumption. Samples just after mixing contained 30% ambient air ($\sim 60 \mu\text{M}$ oxygen), 5 μM CcO, 40 μM cyt c^{2+} , 0.05 M Hepes, 0.2% Tween 20, and 0.167 M K_2SO_4 (ionic strength = 0.5). Modulation, gain and power settings were as indicated for the ^{15}N -perdeuterated probe of Figure 1. Neither sample contained ascorbate. Experimental time constant was 0.01 s. Each trace was the average of 10 transients. The signal averager used 30 ms/address. The inset was obtained by normalizing each trace to 100 units, taking the natural log, and plotting it vs time.

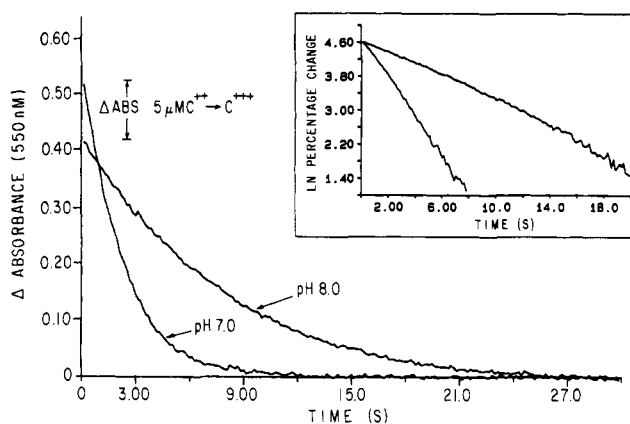


FIGURE 4: Optically detected cyt c^{2+} consumption. Samples just after mixing contained 100% ambient air, 5 μM CcO, 40 μM cyt c^{2+} , 0.05 M Hepes, 0.2% Tween 20, and 0.167 M K_2SO_4 (ionic strength = 0.5). Signal averager used 67 ms/address. The semilogarithmic inset was obtained by taking optical data starting 0.15 s after mixing, normalizing the resultant signal height to 100 units, taking natural logarithms, and plotting vs time.

monitored oxygen consumption. (For following cyt c^{2+} consumption we used 100% ambient air rather than 30%, and CTPO was not generally used in our optically detected stopped-flow experiments, although as a control we determined that 200 μM CTPO had no effect on the cyt c^{2+} kinetics.) Oxygen and cyt c^{2+} consumption were both faster at pH 7.0 than at pH 8.0.

The insets to Figures 3 and 4 show semilogarithmic plots of the respective oxygen and cyt c^{2+} signals after they were normalized to an amplitude of 100%. At present we have simply estimated from the approximately linear behavior of these semilogarithmic plots apparent first-order rate constants. For oxygen these apparent first-order rates were 0.35 s^{-1} at pH 7 and 0.13 s^{-1} at pH 8; for cyt c^{2+} , 0.46 s^{-1} at pH 7.0 and 0.15 s^{-1} at pH 8.0. Thus either apparent first-order rate was ~ 3 times faster at pH 7 than at pH 8. We also estimated initial rates of reactant consumption over the period 0.5–1.0 s, although there is more inherent uncertainty in such initial rates which are determined over a short time range. For

oxygen these initial rates were $1.2 \mu\text{M O}_2/\text{s}$ at pH 7 and $0.7 \mu\text{M O}_2/\text{s}$ at pH 8, and for cyt c^{2+} they were $8.3 \mu\text{M cyt c}^{2+}/\text{s}$ at pH 7 and $2.2 \mu\text{M cyt c}^{2+}/\text{s}$ at pH 8. Both the apparent first-order rates and the initial rates of reactant consumption indicated a tendency of oxygen consumption to lag behind cyt c^{2+} consumption.

The work indicated in Figures 3 and 4 was done without addition of ascorbate to prevent autoxidation of cyt c^{2+} . Others who do such kinetic work often add a small concentration of ascorbate to maintain cyt c^{2+} in reduced form (Thornström et al., 1988). Over a 20-min period, which is about the time needed to perform one set of time-resolved spin-probe oximetry measurements, cyt c^{2+} partially autoxidizes, and so we recognize that the initial concentration of cyt c^{2+} , which is given as $40 \mu\text{M}$ for Figures 3 and 4, is approximate. A complication to using ascorbate is that ascorbate leads to slow regeneration of cyt c^{2+} and concomitant slow continuous consumption of oxygen after the initial charge of cyt c^{2+} is nearly exhausted by the reaction with CcO. The slow regeneration of cyt c^{2+} and its immediate catalysis in the presence of CcO would not be noticed optically, but the concomitant slow consumption of oxygen is especially noticeable at pH 8.0, where we have found the rate of ascorbate-induced regeneration of cyt c^{2+} to be higher than at pH 7.0. Having such a continuous oxygen consumption, especially at pH 8.0, superimposed on the desired oxygen kinetic trace a downward-sloping tail or base line.

Discussion: Oxygen Consumption Limited by Available Cyt c^{2+} . As shown by the kinetic traces of Figure 3, the amount of oxygen consumed can clearly be made comparable with the CcO concentration, in contrast to the usual polarographic experiments where the CcO concentration is much less than the oxygen concentration. Heretofore, the pH dependence in CcO's catalytic activity has been monitored in limited-turnover experiments by following cyt c^{2+} consumption. For example, the half-time for cyt c^{2+} consumption was 3-fold shorter at pH 7.4 than at pH 8.4 (Thornström et al., 1988). The oxygen consumption experiments shown in Figure 3 and the cyt c^{2+} consumption experiments of Figure 4 definitely show kinetic oxygen consumption is pH-dependent like cyt c^{2+} consumption, and the time behavior in oxygen consumption quantitatively parallels the cyt c^{2+} consumption. When our oxygen and cyt c^{2+} transient signals had been normalized and compared on a percentage basis (in preparation for semilogarithmic plotting), the oxygen consumption at both pH 7 and pH 8 appeared very slightly to lag behind the cyt c^{2+} consumption. The pH dependence of CcO's activity has been thought to be the link that connects proton pumping and internal electron transfer between the low-potential cytochrome a and Cu_A sites, which are initially reduced by cyt c^{2+} , and the a_3 - Cu_B center where oxygen is subsequently catalyzed (Malmström, 1985, 1990; Brzezinski & Malmström, 1986). These oximetry experiments provide a new technique for following such pH dependence at a different point in the CcO catalytic cycle. Following the present methodology-oriented work reported here, a more detailed biochemical investigation is ongoing to determine the details of this pH-dependent relation between cyt c^{2+} and oxygen consumption and to determine under what conditions the ratio of the rates of cyt c^{2+} and oxygen consumption differ from the stoichiometrically expected value of 4. Now that the methods for following oxygen consumption over the first 100 ms after mixing have been developed, we also intend to probe the relation between the burst phase of cyt c^{2+} consumption (where cytochrome a and Cu_A are initially reduced) and the immediately subsequent oxygen kinetics. At present, we definitely do not see a burst of oxygen consumption

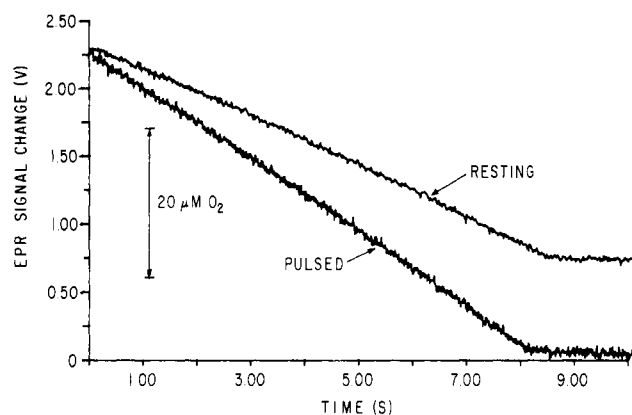


FIGURE 5: Complete oxygen consumption from $\sim 20\%$ air ($40 \mu\text{M}$ oxygen) to no oxygen under conditions where cyt c^{2+} was not a limiting factor because of excess ascorbate and TMPD. Conditions after mixing were $5 \mu\text{M CcO}$, $40 \mu\text{M cyt c}^{2+}$, 1 mM ascorbate , $200 \mu\text{M TMPD}$, 0.05 M Hepes , pH 7, $0.167 \text{ M K}_2\text{SO}_4$, $0.2\% \text{ Tween 20}$, and ^{15}N -perdeuterated probe. "Pulsed" CcO was prepared and premixed as discussed in the text so that it had undergone many turnovers and was anaerobic when mixed with spin probe and $80 \mu\text{M}$ oxygen buffer. "Resting" CcO and the reductants for it were assembled in separate syringes with the oxygen concentration in both syringes at about 20% air ($40 \mu\text{M}$ oxygen). These traces represent the accumulation of 16 transients, each with an experimental time constant of 0.01 s . The signal averager used 30 ms/address . The $20 \mu\text{M}$ oxygen bar represents the change in signal that occurs when there is a $20 \mu\text{M}$ oxygen decrease from an initial starting oxygen concentration of $40 \mu\text{M}$.

in the first 100 ms following mixing, but we are uncertain if there is a lag in oxygen consumption during the time of the burst.

Results: Oxygen Consumption in the Presence of Continuously Regenerated Cyt c^{2+} . Oxygen kinetics were followed with sufficient cyt c^{2+} to completely exhaust all oxygen. To guarantee adequate cyt c^{2+} , we used 1 mM ascorbate and the redox mediator TMPD (Thornström et al., 1988; Hill & Nicholls, 1980) which facilitates rapid electron transfer between ascorbate and cyt c^{3+} . The half-time for complete reduction of $40 \mu\text{M cyt c}^{3+}$ by 1 mM ascorbate and $200 \mu\text{M TMPD}$ was measured by optical stopped flow at 0.15 s .

In Figure 5 the resultant kinetic traces are shown for consumption of approximately $40 \mu\text{M}$ oxygen (20% ambient air). When cyt c^{2+} remained in excess, the rate of oxygen consumption remained essentially constant (i.e., zeroth-order kinetics) until nearly all the oxygen was consumed and the rate and slope went to zero. Such zeroth-order kinetic behavior is seen, but on a longer time scale than the $\sim 8 \text{ s}$ of our measurements, with polarographic or phosphorescence techniques (Vanderkooi et al., 1987; Wilson et al., 1988). Such general kinetic behavior was previously noted during cellular respiration (Froncisz et al., 1985). In Figure 5 the ratio of oxygen consumed to CcO enzyme was about 8, a number much smaller and more finite than in previous measurements.

Figure 5 showed a difference in oxygen-consuming behavior between "pulsed" and "resting" enzyme. Since "resting" enzyme will convert to "pulsed" after many turnovers (Antonini et al., 1985), an important advantage of our technique was that it limited the number of oxygen turnovers per oxidase molecule. To make the prereduced "pulsed" enzyme, we first combined CcO, cyt c^{3+} , ascorbate, and TMPD in one syringe and allowed all the oxygen to be consumed in that syringe. The other syringe contained spin probe and approximately $80 \mu\text{M}$ dissolved oxygen. Then we rapidly mixed the two solutions so that immediately after mixing there was an oxygen concentration of $40 \mu\text{M}$ oxygen (20% ambient air) to be consumed by "pulsed" enzyme. To perform the corresponding experiment

with "resting" enzyme, we prepared two separate solutions, each containing $40\ \mu\text{M}$ oxygen. The first solution contained "resting" CcO and spin probe; the other contained the reductants $\text{cyt } c^{2+}$, ascorbate, and TMPD. Then the two solutions were rapidly mixed to start the reaction in the presence of "resting" enzyme. Because we needed to ensure that no bubbles were transferred from the reaction syringe to the storage syringe, it was difficult to precisely control the starting oxygen concentrations in the two types of experiments so that the oxygen concentrations just after mixing would be an identical $40\ \mu\text{M}$. However, the critical point in the experiments comparing "resting" and "pulsed" enzyme was that the rates of oxygen consumption (i.e., slopes of the curves) were different at the same oxygen concentration and not whether the starting amount of oxygen was exactly the same or whether the exact overall oxygen consumed was the same for "resting" and "pulsed" enzymes. Using our calibration expression (eq 1 and its derivative), we determined that the oxygen consumption rate for "pulsed" enzyme was $4.5 \pm 0.5\ \mu\text{M O}_2/\text{s}$ and the rate for "resting" enzyme was $3.7 \pm 0.5\ \mu\text{M O}_2/\text{s}$. At pH 7.0 the rate of oxygen consumption in these experiments with TMPD present was 2–4 times larger than in the initial second of the limited $\text{cyt } c^{2+}$ experiments above.

As oxygen was being completely consumed, we observed that its rate of consumption fell to zero as indicated by the flat base line. Under the conditions similar to Figure 5, the time where oxygen concentration became rate limiting occurred 7–8 s after mixing, and the rate of oxygen consumption approached zero over a period of less than a second. Oxygen becomes rate limiting at oxygen concentrations below $1\ \mu\text{M}$ (Vanderkooi et al., 1987; Wilson et al., 1988). According to our calibration, a $1\ \mu\text{M}$ oxygen concentration change that occurs as oxygen becomes rate limiting will give about a 65-mV signal change for the ^{15}N -perdeuterated probe, to be compared with about 30-mV p.t.p. noise. Thus for a detailed presentation in time of the rate-limiting phenomenon, it was necessary to do repetitive signal averaging, triggered a few hundred milliseconds before the onset of anaerobic behavior. We collected 10 transients at an EPR experimental time constant of 0.01 s and an address time of 0.002 s and then digitally smoothed at an effective time constant of 0.02 s. The results of this experiment for $5\ \mu\text{M}$ CcO are shown in Figure 6A. We define $P_{1/2}$ as the oxygen concentration where the rate of oxygen consumption went to half its maximal value, and we graphically estimated that $P_{1/2}$ is at $0.3 \pm 0.1\ \mu\text{M}$ oxygen above the base line. We also empirically least-squares fit the curve of Figure 6A to an integrated Michaelis–Menten expression (Froncisz et al., 1985; Cornish-Bowden, 1976), and this fit gave a value of $P_{1/2} = 0.4\ \mu\text{M}$. As oxygen was being consumed by $1\ \mu\text{M}$ CcO, but otherwise the same reactant conditions, the oxygen-limiting behavior, commencing about 45 s after mixing, is shown in Figure 6B. Oxygen limitation in Figure 6B occurred at a $P_{1/2} \leq 0.1\ \mu\text{M}$ oxygen above the base line. The respective $P_{1/2}$ values shown by the data in Figure 6, panels A and B, were dependent on the CcO concentration but not on whether the CcO started in the "resting" or the "pulsed" form.

Discussion: Oxygen Consumption in the Presence of Continuously Regenerated $\text{Cyt } c^{2+}$. These experiments showed that rapid oxygen consumption, exhibiting a different time course from the limited $\text{cyt } c^{2+}$ experiments above, could also be followed. Because the rate-limiting step in oxygen consumption is not oxygen dependent above $1\ \mu\text{M}$ oxygen, these experiments exhibited zeroth-order kinetics until very low oxygen concentrations. When $\text{cyt } c^{2+}$ was kept continuously

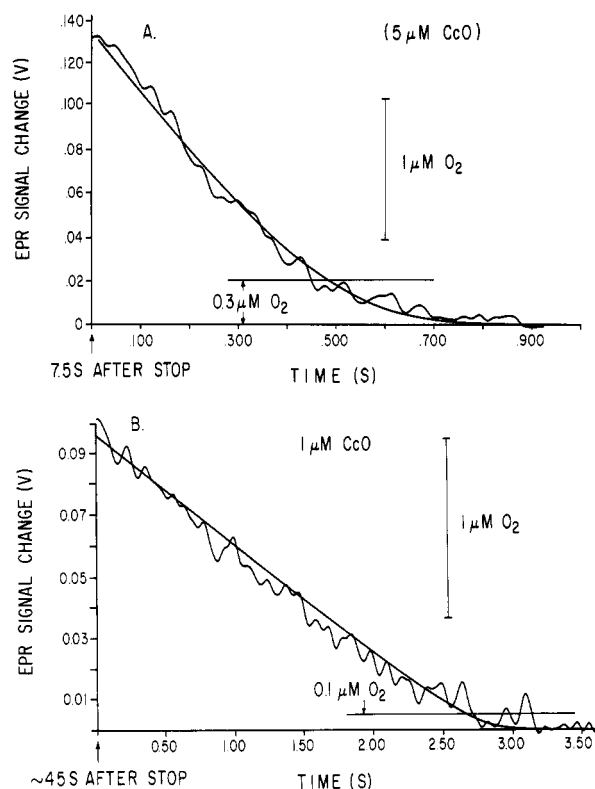


FIGURE 6: Panel A shows the details of oxygen consumption by $5\ \mu\text{M}$ CcO near the point in time, which was about 7.5 s after mixing, where oxygen became rate limiting in Figure 5. The solution following mixing of "pulsed" oxidase with oxygen-containing buffer contained $5\ \mu\text{M}$ CcO, $40\ \mu\text{M}$ $\text{cyt } c^{2+}$, $1\ \text{mM}$ ascorbate, $200\ \mu\text{M}$ TMPD, $0.05\ \text{M}$ Hepes, $0.167\ \text{M}$ K_2SO_4 , pH 7.0, and $200\ \mu\text{M}$ ^{15}N -perdeuterated spin probe. The signal averager was triggered $\sim 0.5\ \text{s}$ before the rate of EPR signal change went to zero. Ten transients were collected with an instrumental time constant of 0.01 s, the signal averager used 2 ms/address, and the data were smoothed with a 10-address smooth. The line $0.3\ \mu\text{M}$ above the base line is our graphic estimate of the $P_{1/2}$ value where the slope went to $1/2$ its initial value. The solid line is the result of a least-squares fit to an integrated Michaelis–Menten equation that indicated $P_{1/2} = 0.4\ \mu\text{M}$. Panel B shows the details of oxygen consumption by $1\ \mu\text{M}$ CcO near the point in time where oxygen became rate limiting. Other than the CcO concentration, the reactants were identical to those for panel A. The line $0.1\ \mu\text{M}$ above the base line is our graphical estimate of $P_{1/2}$ where the slope to $1/2$ its initial value, and the solid line is the result of a least-squares fit to an integrated Michaelis–Menten equation that indicated $P_{1/2} = 0.1\ \mu\text{M}$. A calibration factor of $65\ \text{mV} = 1\ \mu\text{M}$ oxygen (see Experimental Procedures) was used in relating voltage change to oxygen concentration.

replenished by ascorbate and TMPD, its concentration as observed optically remained at a steady level. It has been suggested that TMPD is effective in reducing $\text{cyt } c^{3+}$ still bound to CcO (Hill & Nicholls, 1980; Cooper, 1990). Thus the release of oxidized $\text{cyt } c^{3+}$ from its oxidase binding site would not impede the catalytic cycle of CcO as it might in the limited $\text{cyt } c^{2+}$ experiments above where there was no TMPD.

The ratio of oxygen to be consumed to $5\ \mu\text{M}$ enzyme, though larger than in the $\text{cyt } c^{2+}$ limited experiments, was finite, and differences could be observed between oxygen consumption by CcO prepared as "resting" or as "pulsed" enzyme, apparently because the "resting" enzyme did not turn over rapidly enough or frequently enough to convert to "pulsed" (Antonini et al., 1985). Following these initial experiments we intend to vary the enzyme and substrate conditions to determine if we can resolve an even larger "resting – pulsed" difference and to see if pH-dependent differences in the zeroth-order rate are consistent with the pH differences observed in oxygen consumption under $\text{cyt } c^{2+}$ limited turnover, implying

that the differences reflect the same rate-limiting step.

As shown in Figure 6, the time-resolved spin-probe oximetry technique also gave information on the approach to nearly anaerobic oxygen consumption as oxygen became exhausted. At this point the kinetics were no longer zeroth-order in oxygen concentration, and the oxygen concentration was considerably less than the enzyme concentration. The approach to anaerobic behavior had to be followed over a shorter time regime than previously used to follow such oxygen-limited kinetics (Vanderkooi et al., 1987; Wilson et al., 1988). Although Froncisz et al. (1985) explicitly reported that such signals can be used for linearly measuring oxygen concentrations down to 0.1 μM , an experimental concern in interpreting our oximetry measurements at very low oxygen concentrations might be that we had not calibrated the 90°-out-of-phase dispersion EPR signal at such low (<1 μM) oxygen concentrations. In graphically estimating the $P_{1/2}$ of 0.3 μM for Figure 6A, for example, we were in fact assuming that the spin-probe response was linear (at 65 mV/ μM O_2) in oxygen concentration below 1 μM . If the phenomenon that we were observing were a technical artifact of our probe method at very low oxygen concentrations, we would not expect that the oxygen concentration, i.e., $P_{1/2}$, which is rate-limiting would be dependent on oxidase concentration. We therefore have strong evidence that we are observing the onset of rate-limiting behavior and that there is a difference between 5 and 1 μM enzyme in the oxygen concentration where oxygen-limited behavior starts. However, the precise value of the $P_{1/2}$'s that we estimate could be in error if there were nonlinearity in the response of the probe signal to oxygen below 1 μM oxygen.

Time-resolved spin-probe oximetry has given us a new tool for observing the way in which oxygen itself becomes rate limiting on a rapid time scale not previously followed, and it has provided the experimental motivation for examining the theory of oxygen consumption by CcO at very low oxygen concentrations. We wondered if the dependence of $P_{1/2}$ on enzyme concentration was peculiar to CcO or if it could be an example of a general kinetic phenomenon that occurs whenever the concentration of a critical rate-limiting enzyme intermediate could no longer be considered at steady state (Cornish-Bowden, 1976). The commonly used steady-state Michaelis-Menten approach, where $d[\text{O}_2]/dt = V_{\text{max}}[\text{O}_2]/(K_m + [\text{O}_2])$, would tell us that $P_{1/2}$ is the K_m value for $[\text{O}_2]$. It is this equation for $d[\text{O}_2]/dt$ which when integrated gave the fitted curves of Figure 6. In the limit of a very small enzyme concentration and a steady-state level of the critical, rate-limiting enzyme-substrate complex (commonly called ES), $P_{1/2}$ or K_m should be independent of enzyme concentration. It is, of course, not clear in a limited-turnover experiment, where the enzyme concentration and the substrate concentration ($[\text{O}_2]$ here) are comparable, that the steady-state approximation, $d(\text{ES})/dt = 0$, ought to be valid. The Michaelis-Menten equations were again applied, but with no steady-state approximation [i.e., $d(\text{ES})/dt \neq 0$]. After using Runge-Kutta methods to solve the coupled, non-steady-state Michaelis-Menten differential equations, we found that $P_{1/2}$ could indeed be made dependent on enzyme concentration.

The more complex kinetic equations of Brzezinski et al. (1986) were designed to describe the consumption of cyt c^{2+} by CcO in a more fundamental fashion than phenomenological Michaelis-Menten equations. Our long-range goal is to apply these equations [or updated versions of them that include proton-coupled electron transfer, as in Thronström et al. (1988)] to comprehensively explain cyt c^{2+} and oxygen consumption by CcO. These equations include detailed steps for

cyt c^{2+} binding, electron transfer to cytochrome *a* and Cu_A , a potentially rate-limiting electron-transfer step from cytochrome *a* and Cu_A to the a_3 - Cu_B center, and an oxygen-consuming step. Here we report that the equations of Brzezinski et al. (1986) could be made to explain adequately our measured oxygen consumption under conditions of excess cyt c^{2+} . We included in them an additional term for regeneration of cyt c^{2+} , took kinetic parameters used by Brzezinski et al. (1986), and solved the equations by Runge-Kutta methods. We found a zeroth-order rate law for oxygen consumption to below 1 μM oxygen, and $P_{1/2}$ was predicted to depend on enzyme concentration.

CONCLUSION

We have combined rapid-mixing, stopped-flow EPR with spin-probe oximetry to follow oxygen consumption by the enzyme CcO. We have applied this technique to microliter volumes of enzyme at micromolar concentrations of enzyme and oxygen. In a fashion continuous in time we have followed micromolar oxygen concentration changes where the amount of oxygen consumed was comparable with or even less than the amount of enzyme. The combination of stopped-flow EPR and spin-probe oximetry has given time resolution of the order of 30 ms after mixing to determine even submicromolar concentration changes of oxygen. The experiments where we have followed oxygen consumption have been done under the following two limiting conditions: (1) where the amount of cyt c^{2+} was limited and the time course of oxygen consumption and its pH dependence bore resemblance to optically detected cyt c^{2+} consumption; (2) where the amount of oxygen itself was limited but cyt c^{2+} was regenerated so that the kinetics of oxygen consumption showed a zeroth-order rate dependence down to an oxygen concentration of less than 1 μM . The kinetics as oxygen concentration became rate limiting could be observed over a period of less than a second, and the characteristic oxygen concentration where oxygen itself became rate limiting could be estimated. This work points the way for future rapid kinetic studies of the rate of oxygen consumption under limited-turnover conditions.

ACKNOWLEDGMENTS

We are indebted to Dr. W. Z. Plachy for suggesting the ^{15}N -perdeuterated CTPO; to Mr. Harold Taylor for electronic repairs, development of the high-pass filter, and incorporation of the GASFET amplifier; and to Ms. Jessica W. Wolpaw for valuable contributions in the testing and development stages.

REFERENCES

- Antonini, E., Brunori, M., Colosimo, A., Greenwood, C., & Wilson, M. T. (1977) *Proc. Natl. Acad. Sci. U.S.A.* 74, 3128-3132.
- Antonini, G., Brunori, M., Colosimo, A., Malatesta, F., & Sarti, P. (1985) *J. Inorg. Biochem.* 23, 289-293.
- Babcock, G. T., Jean, J. M., Johnston, L. N., Palmer, G., & Woodruff, W. H. (1984) *J. Am. Chem. Soc.* 106, 8305-8306.
- Brzezinski, P., & Malmström, B. G. (1986) *Proc. Natl. Acad. Sci. U.S.A.* 83, 4282-4286.
- Brzezinski, P., Thronström, P.-E., & Malmström, B. G. (1986) *FEBS Lett.* 194, 1-5.
- Chance, B., Saronio, C., & Leigh, J. S. (1975) *J. Biol. Chem.* 250, 9226-9237.
- Cooper, C. E. (1990) *Biochim. Biophys. Acta* 1017, 187-203.
- Cornish-Bowden, A. (1976) *Principles of Enzyme Kinetics*, pp 16-23 and 142-144, Butterworths & Co., London.

- Davies, P. W. (1962) in *Physical Techniques in Biological Research* (Nastuk, W. L., Ed.) Vol. 4, pp 137-179, Academic Press, New York.
- Fan, C., Bank, J. F., Dorr, R., & Scholes, C. P. (1988) *J. Biol. Chem.* 263, 3588-3591.
- Francisz, W., & Hyde, J. S. (1982) *J. Magn. Reson.* 47, 515-521.
- Francisz, W., Lai, C.-S., & Hyde, J. S. (1985) *Proc. Natl. Acad. Sci. U.S.A.* 82, 411-415.
- Gibson, Q. H., & Greenwood, C. (1963) *Biochem. J.* 86, 541-554.
- Gibson, Q. H., Swoboda, B. E. P., & Massey, V. (1964) *J. Biol. Chem.* 239, 3927-3934.
- Han, S., Ching, Y.-C., & Rousseau, D. L. (1990) *Proc. Natl. Acad. Sci. U.S.A.* 87, 8408-8412.
- Hendler, R. W., Subba Reddy, K. V., Shrager, R. I., & Caughey, W. S. (1986) *Biophys. J.* 49, 717-729.
- Hill, B. C., & Nicholls, P. (1980) *Biochem. J.* 187, 809-818.
- Hill, B. C., & Greenwood, C. (1983) *Biochem. J.* 215, 659-667.
- Hubbell, W. L., Francisz, W., & Hyde, J. S. (1987) *Rev. Sci. Instrum.* 58, 1879-1886.
- Jensen, P., Aasa, R., & Malmström, B. G. (1981) *FEBS Lett.* 125, 161-164.
- Kuboyama, M., Yong, F. C., & King, T. E. (1972) *J. Biol. Chem.* 247, 6375-6383.
- Lai, C.-S., Hopwood, L. E., Hyde, J. S., & Lukiewicz, S. (1982) *Proc. Natl. Acad. Sci. U.S.A.* 79, 1166-1170.
- Malmström, B. G. (1985) *Biochim. Biophys. Acta* 811, 1-12.
- Malmström, B. G. (1990) *Arch. Biochem. Biophys.* 280, 233-241.
- Malmström, B. G., & Nilsson, T. (1988) in *Cytochrome Oxidase: Structure, Function and Physiopathology* (Brunori, M., & Chance, B., Eds.) *Ann. N.Y. Acad. Sci.* 550, 177-184.
- Martin, C. T., Scholes, C. P., & Chan, S. I. (1985) *J. Biol. Chem.* 260, 2857-2861.
- Mascarenhas, R., Wei, Y.-H., Scholes, C. P., & King, T. E. (1983) *J. Biol. Chem.* 258, 5348-5351.
- Morse, P. D. (1987) *Biophys. J.* 51, 440a.
- Ogura, T., Takahashi, S., Shinzawa-Itoh, K., Yoshikawa, S., & Kitagawa, T. (1990) *J. Biol. Chem.* 265, 14721-14723.
- Povich, M. J. (1975) *J. Phys. Chem.* 79, 346-351.
- Scholes, C. P., Bank, J. F., Fan, C., & Taylor, H. (1987) in *Advances in Membrane Biochemistry and Bioenergetics* (Kim, C. H., Tedeschi, H., Diwan, J. J., & Salerno, J. C., Eds.) pp 439-447, Plenum Press, New York.
- Stevens, T. H., Martin, C. T., Wang, H., Brudvig, G. W., Scholes, C. P., & Chan, S. I. (1982) *J. Biol. Chem.* 257, 12106-12113.
- Strzalka, K., Walczak, T., Sarna, T., & Swartz, H. M. (1990) *Arch. Biochem. Biophys.* 281, 312-318.
- Subczynski, W. K., & Hyde, J. S. (1981) *Biochim. Biophys. Acta* 643, 283-291.
- Swartz, H. M., & Glockner, J. F. (1989) in *Advanced EPR in Biology and Biochemistry* (Hoff, A. J., Ed.) pp 753-782, Elsevier Science Publishers, Amsterdam.
- Thornström, P.-E., Brzezinski, P., Fredriksson, P.-Ö., & Malmström, B. G. (1988) *Biochemistry* 27, 5441-5447.
- Vanderkooi, J. M., Maniara, G., Green, T. J., & Wilson, D. F. (1987) *J. Biol. Chem.* 262, 5476-5482.
- Wilson, D. F., Rumsey, W. L., Green, T. J., & Vanderkooi, J. M. (1988) *J. Biol. Chem.* 263, 2712-2718.
- Wikström, M., Krab, K., & Saraste, M. (1981) in *Cytochrome Oxidase A Synthesis*, Chapter 7, pp 142-170, Academic Press, London.
- Windrem, D. A., & Plachy, W. Z. (1980) *Biochim. Biophys. Acta* 600, 655-665.
- Yu, C. A., Yu, L., & King, T. E. (1975) *J. Biol. Chem.* 250, 1383-1392.